Superlattices and Microstructures 47 (2010) 586–591

Contents lists available at ScienceDirect

Superlattices and Microstructures

journal homepage: www.elsevier.com/locate/superlattices

The effect of hydrostatic pressure on the electrical characterization of Au/*n*-InP Schottky diodes

N. Ucar [a,*], A.F. Ozdemir [a], D.A. Aldemir [a], S. Cakmak [a], A. Calik [b], H. Yildiz [a], F. Cimilli [c]

[a] *Physics Department, Art and Science Faculty, Suleyman Demirel University, Isparta, Turkey*

[b] *Department of Mechanical Education, Technical Education Faculty, Suleyman Demirel University, Isparta, Turkey*

[c] *Physics Department, Art and Science Faculty, Atatürk University, Erzurum, Turkey*

ARTICLE INFO

Article history:
Received 23 October 2009
Received in revised form
13 January 2010
Accepted 18 February 2010
Available online 12 March 2010

Keywords:
Schottky barrier diode
Barrier height
Hydrostatic pressure
Ideality factor
Interface states
Fermi level pinning

ABSTRACT

The effect of hydrostatic pressure on the interface state density and Schottky barrier diode parameters such as ideality factor and barrier height obtained from the current–voltage (I–V) characteristics of Au/n-InP Schottky diodes was studied. It is shown that the ideality factor and the barrier height values of Au/n-InP diodes are in the range 2.36–1.93 and 0.546–0.579 eV for the 0.0–5.0 kbar pressure interval at room temperature, respectively. We have seen that the barrier height for Au/n-InP Schottky diodes has a linear pressure coefficient of 6.87 meV/kbar (=68.7 meV/GPa), approximately equal to that found for the band gap of InP. This means that the Fermi level is a reference level which is pinned to the conduction band minimum as a function of pressure. On the other hand, the interface state density decreases with increasing hydrostatic pressure due to the rectifying properties of the diode.

© 2010 Elsevier Ltd. All rights reserved.

1. Introduction

Schottky barrier diodes (SBDs) have been widely studied in terms of material and device physics, design and fabrication technology and applications for decades. The most characteristic parameter of these diodes is their barrier height (Φ_b); that is, the energy separation between the Fermi level and the edge of the majority carrier band right at the interface [1–3]. However, a serious limitation of InP SBDs is the low Φ_b and large leakage currents which may be due to Fermi level pinning [4]. So, the low-Φ_b Schottky diodes of n-InP seem to be a good candidate for the application of zero-bias Schottky detector diodes [4–6].

* Corresponding author. Tel.: +90 2462114017.
E-mail address: nucar@fef.sdu.edu.tr (N. Ucar).

0749-6036/$ – see front matter © 2010 Elsevier Ltd. All rights reserved.
doi:10.1016/j.spmi.2010.02.003

In a metal/semiconductor system, the Fermi level within the semiconductor band gap determines the formation of Φ_b, and thus the exact position of the Fermi level depends on the details of the interface [7–9]. On the other hand, the Φ_b of metal/semiconductor contacts is almost independent of the metal work function. Such a behavior indicates that some mechanisms must be responsible for the Fermi level pinning, such as metal-induced gap states (MIGSs) and defect models [10,11]. Thus, it has been shown that the investigation of the temperature dependence of Φ_b is very helpful for understanding the problem of Fermi level pinning. Corresponding to this, Kumar et al. [12] showed that the zero-bias Schottky barrier height decreases with decreasing temperature. However, the flat-band barrier height is almost independent of the temperature in Au/*n*-Si Schottky diodes. These results have been interpreted by using the models of Fermi level pinning.

Recently, hydrostatic pressure as well as the temperature dependence of SBDs has been investigated in order to study the optical and electrical properties and Schottky barrier formation. It is well known that these properties are sensitive to the application of external pressure and to the variations in temperature as well as non-idealities such as the interface state, interface oxide layer, interface fixed charges, interface traps and series resistance [13–15]. So, in recent years, hydrostatic pressure has been used as a tool for studying the optical and electronic properties of semiconductors and SBDs. The experimental evidence shows that pressure or stress plays a very important role in the transport properties in semiconductor materials [16]. The well-known effects are the energy band gap variation with hydrostatic pressure, the stress-induced piezoelectric field in III–V compound semiconductors, and the change of the band edge curvature and the band edge splitting with uniaxial pressure [17]. In this connection, it has been shown that Φ_b decreases under compressive stress parallel to the interface and increases under tensile stress due to the change in band gap caused by stress [18]. Additionally, Cankaya and Abay [13] showed that Φ_b, the ideality factor (n) and the series resistance (R_S) of Cd/*p*-GaTe SBDs decrease with an increase in the hydrostatic pressure. In contrast, Sonmezoglu et al. [19] showed that the values of Φ_b and n of Cd/*n*-GaAS SBDs increase with increasing hydrostatic pressure. So, it can be said from the experimental results on ideal Schottky diodes that the Fermi level is pinned relative to the valence band or conduction band edge at the interface to explain both the temperature and applied pressure dependence of Φ_b. Considering the Fermi level pinning and interface properties of metal/semiconductor systems, it would be interesting to study the hydrostatic pressure effect on the Au/*n*-InP SBD parameters such as Φ_b, and also interface state density (N_{SS}), and this paper presents our important results on them by using current–voltage (I–V) measurements.

2. Experimental method

The *n*-type InP wafer (Si-doped) used was (100) oriented with a free carrier concentration of $(2.90 \pm 0.05) \times 10^{15}$ cm^{-3} at room temperature. The wafer was degreased consecutively in trichloroethylene, acetone and methanol for 3 min. The degreased wafer was etched with H_2SO_4:H_2O_2:H_2O (5:1:1) for 1 min to remove surface damage and undesirable impurities. Indium was evaporated on the backside of the *n*-InP to provide the ohmic contact and the *n*-InP/In structure was annealed at 350 °C for 2 min in a N_2 atmosphere. Schottky contacts were formed on the front face of the *n*-InP as dots with a diameter of about 1 mm by evaporation of Au.

The pressure was created by a piston and cylinder-type chamber apparatus and a special transformer oil was used to transmit the pressure. The Au/*n*-InP Schottky diode was located in the pressure cell by using a specially designed sample holder and the I–V measurements in the hydrostatic pressure range of 0 to 5 kbar were made by electrical connections from the cell to the diode. The I–V characteristics of the Au/*n*-InP Schottky diodes with pressure and without pressure were obtained using an HP 4140B picoammeter in complete darkness and at room temperature.

3. Results and discussion

For SBDs, the thermionic emission theory predicts that the I–V characteristics are given as follows [20–22]:

$$I = I_S \left(\frac{qV}{nkT}\right)\left[1 - \exp\left(-\frac{qV}{kT}\right)\right]. \tag{1}$$

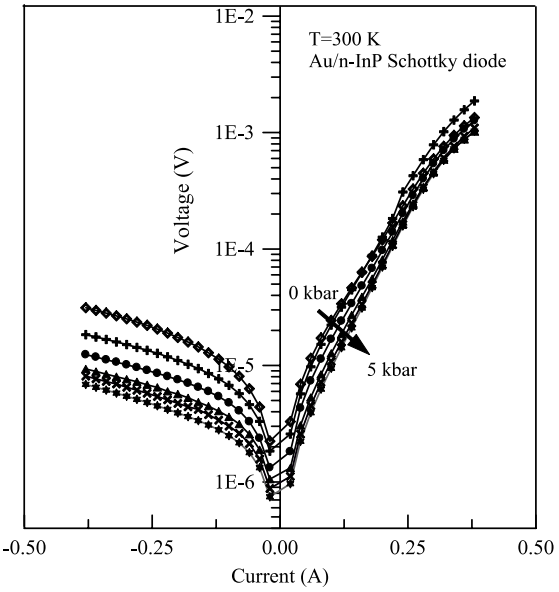


Fig. 1. Current–voltage characteristics of Au/n-InP Schottky diodes under hydrostatic pressure.

In Eq. (1), I_S is the saturation current derived from the straight line intercept of $\ln I$ at $V = 0$, and it is given by

$$I_S = A\overset{*}{A}T^2 \exp\left[\frac{-q\Phi_b}{kT}\right]. \tag{2}$$

$\overset{*}{A}$ is the effective Richardson constant of 9.24 A/cm^2 K^2 for n-InP [23]. Φ_b is the zero bias barrier height, and n is an ideality factor which can be determined accurately from the slope of the linear portion of the $\ln(1/(1 - \exp(-qV/kT)))$ versus V plot given in Fig. 1, and from Eq. (1). In fact, n can be written as

$$n = \frac{q}{kT}\left[\frac{\partial V}{\partial(\ln I)}\right]. \tag{3}$$

Fig. 1 shows the semi-logarithmic forward and reverse bias I–V characteristics of Au/n-InP Schottky diodes as a function of different pressure values ($P = 0$ to 5 kbar). As seen in this figure, the current of the Au/n-InP Schottky diodes decreases with increasing hydrostatic pressure due to an increase of the Schottky barrier height. The values of Φ_b of Au/n-InP Schottky diodes were calculated with the help of Eqs. (2) and (3) from the y-axis intercepts of the experimental semi-log forward bias I–V characteristics, indicating that the effect of series resistance in this region was not important [24]. These values are given in Table 1. As seen in Table 1 and Fig. 1, n decreases with the increasing hydrostatic pressure. So, we say that the diode quality improves with increasing hydrostatic pressure. But, the n values obtained indicate that the diodes obey a metal–interface layer–semiconductor configuration rather than that of an ideal SBD. For an ideal SBD, $n = 1$. The n values obtained are considerably larger. $n > 1$ has been ascribed to the presence of a bias-dependent Schottky barrier height, interface states at the thin oxide layer between the metal and semiconductor or generation–recombination currents within the space region [20,25–27].

It is well known that, for an ideal Schottky contact, Φ_b decreases with temperature; this is essentially due to the change in the band gap [20]. On the other hand, it has been shown that Φ_b also increases with increase in radiation dose and the presence of fixed negative charges in the oxide layer close to the n-InP surface in Au/n-GaAs [28] and Cu/n-InP [29] Schottky diodes, respectively. In

Table 1
Diode parameters obtained from the I–V characteristics of Au/n-InP Schottky diodes under hydrostatic pressure.

P (kbar)	n	Φ_b (eV)
0	2.36	0.546
1	2.15	0.554
2	2.09	0.560
3	2.06	0.569
4	1.98	0.575
5	1.93	0.579

the present study, the Φ_b values range from 0.546 eV (at $P = 0.0$ kbar) to 0.579 eV ($P = 5.0$ kbar). Thus the Φ_b value has increased by 0.033 to 0.579 eV at 5.0 kbar (Table 1). The variation in Φ_b with pressure was fitted the equation

$$\Phi_b(P) = \Phi_b(0) + \alpha P$$

with $\alpha = 6.87$ meV/kbar (=68.7 meV/GPa) the pressure coefficient of Φ_b (see Fig. 2). In early studies, the pressure coefficients of Au/n-GaAs, Cd/p-GaTe and Sn/p-Si have been found to be 11.21 meV/kbar [30], −8.77 meV/kbar [13] and 5.16 meV/kbar [31], respectively. These values are the same as that of the fundamental gap of the indicated Schottky diodes. So, it has been concluded that the variation of the zero-charge-transfer barrier height due to applied pressure follows precisely the variation of the semiconductor band gap. This trend has been explained with the MIGS model [30, 32]. According to the MIGS model of ideal semiconductor contacts, the analysis of pressure or temperature variation of the barrier heights at metal/semiconductor interfaces indicates the existence of a reference level which is pinned to the valence band maximum or conduction band minimum as a function of pressure or temperature. In our study, the barrier height increases with increasing pressure with a linear pressure coefficient of 68.7 meV/GPa. The calculated and experimental linear pressure coefficients of the band gaps for InP change in the range 75–84 meV/GPa [33–35]. The value obtained in this study is in close agreement with the value reported by these researchers. The difference in the pressure coefficients may change with sample quality, such as the presence of below-band-gap absorption due to defects and/or impurities, as indicated in [36]. Thus, we say that the Fermi level is a reference level which is pinned to the valence band maximum as a function of pressure. That is, the slight increase in the barrier height with increasing pressure is related to the increase in the band gap.

Now let us consider the relation between the interface state density and hydrostatic pressure in Au/n-InP Schottky diodes. It is well known that for a metal/semiconductor diode having interface states in equilibrium with the semiconductor, the ideality factor, n, becomes greater than unity [37]. Diodes with large ideality factor values are far from ideal due to presence of a thick insulator layer between the metal and the semiconductor, and high interface states. Thus, the expression for the density of interface states as deduced by Card and Rhoderick [38] is reduced to

$$N_{SS}(V) = \frac{1}{q}\left[\frac{\varepsilon_i}{\delta}(n(V) - 1) - \frac{\varepsilon_s}{W}\right]$$

where ε_s and ε_i are the permittivity of the semiconductor and the permittivity of the interfacial layer, respectively, δ is the thickness of the insulator layer, and W is the width of the space charge region. The insulator layer thickness was found to be 26.1 Å using the equation for insulator layer capacitance ($C_{0x} = \varepsilon_i A\varepsilon_0/\delta$), where $\varepsilon_i = 3.5\varepsilon_0$ [21,39] and ε_0 is the permittivity of free space. Finally, in n-type semiconductors, the energy of the interface states (E_{SS}) with respect to the top of the conduction band at the surface of the semiconductor is given by [40,41]

$$E_C - E_{SS} = q(\Phi_b - V)$$

where V is the applied voltage drop across the depletion layer and Φ_b is the effective barrier height. The energy distribution of interface states under different hydrostatic pressure is shown in Fig. 3. As can be seen from Fig. 3, the interface state density increases with bias from the midgap towards the top of the conduction band for each hydrostatic pressure value. The values obtained for N_{SS} of Au/n-InP are the same order as those reported in [42,43].

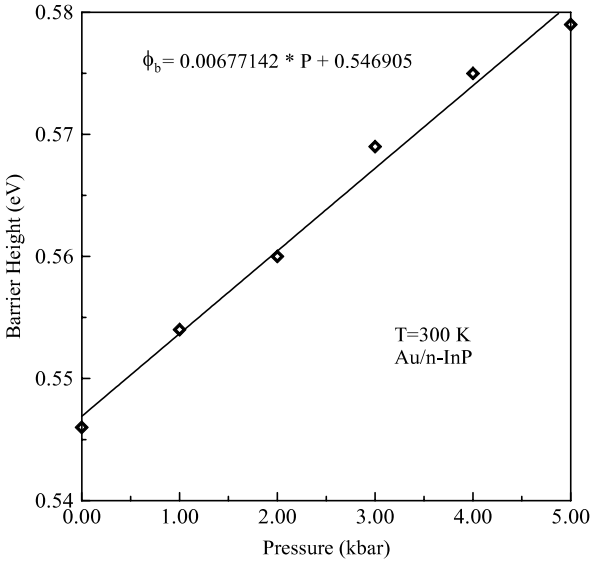


Fig. 2. The change of barrier height of Au/*n*-InP Schottky diodes as a function of hydrostatic pressure.

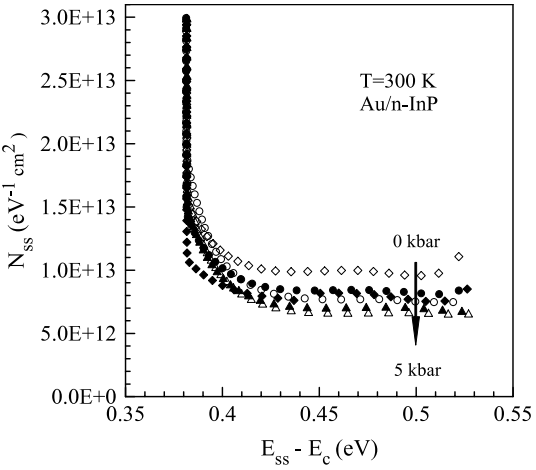


Fig. 3. Density of interface states of Au/*n*-InP Schottky diodes as a function of $E_{SS} - E_C$ obtained from the *I*–*V* characteristics at different hydrostatic pressures.

Also, it is seen that, at around $(E_C - 0.375)$ eV, there was no pressure dependence of the interface state density. On the other hand, N_{SS} decreases with increasing hydrostatic pressure. The same behavior has also been observed between temperature and N_{SS} in the PtSi/*n*-Si [44], Ti/*p*-Si Ge [45] and PtSi/*p*-Si [46] Schottky diodes. This result has been explained with variation of the ideality factor as a function of temperature due to lateral inhomogeneities of the barrier height at the metal/semiconductor interface. Thus, we say that the temperature and hydrostatic pressure have the same effect on the diodes in terms of N_{SS}.

4. Conclusion

The results obtained from *I*–*V* characteristics of Au/*n*-InP diodes showed that the pressure treatment improves the rectifying properties of the diodes. The barrier height increases with

increasing hydrostatic pressure and the Fermi level is a reference level which is pinned to the valence band maximum as a function of pressure. The interface state density under different hydrostatic pressure displays an exponential rise with bias from the midgap towards the bottom of the conduction band. Moreover, N_{SS} decreases with increasing hydrostatic pressure due to the decreasing ideality factor.

References

[1] S. Asubay, O. Gullu, A. Turut, Vacuum 83 (2009) 1470–1474.
[2] R.H. Williams, G.Y. Robinson, in: C.W. Wilmsen (Ed.), Physics and Chemistry of III–V Compound Semiconductor Interfaces, Plenum Press, New York, 1985.
[3] K. Potje-Kamloth, Chem. Rev. 108 (2008) 367–399.
[4] M.B. Reddy, A.A. Kumar, V. Janardhanam, V.R. Reddy, P.N. Reddy, Current Appl. Phys. 9 (2009) 972–977.
[5] Zs.J. Horváth, V. Rakovics, B. Szentpáli, S. Püspöki, Phys. Status Solidi C 3 (2003) 916–921.
[6] P.G. McCafferty, A. Sellai, P. Dawson, H. Elasd, Solid-State Electron. 39 (1996) 583–592.
[7] S. Chand, S. Bala, Phys. B 390 (2007) 179–184.
[8] H. Bayhan, C. Ercelebi, Semicond. Sci. Technol. 12 (1997) 600–608.
[9] T.U. Kampen, W. Mönch, Surf. Sci. 490 (1995) 331–333.
[10] J.H. Werner, H.H. Gü ttler, J. Appl. Phys. 69 (1991) 1522–1533.
[11] J. Osvald, Z.J. Horvath, Appl. Surf. Sci. 234 (2004) 349–354.
[12] S. Kumar, Y.S. Katharria, S. Kumar, D. Kanjilal, Solid-State Electron. 50 (2006) 1835–1837.
[13] G. Cankaya, B. Abay, Semicond. Sci. Technol. 21 (2006) 124–130.
[14] M. Peanasky, Drickamer, Appl. Phys. 56 (1984) 3471–3475.
[15] G. Cankaya, N. Ucar, A. Turut, Phys. Status Solidi a 179 (2000) 469–473.
[16] W. Zhang, C. Xue, J. Xiong, B. Xie, T. Wei, Y. Chen, Indian J. Pure Appl. Phys. 45 (2007) 294–298.
[17] S.C. Jain, M. Wilander, H. Maes, Semicond. Sci. Technol. 11 (1996) 641–671.
[18] M. Kusaka, M. Okamura, N. Hiraoka, M. Hirai, S. Okazaki, Surf. Sci. 86 (1979) 841–847.
[19] S. Sonmezoglu, F. Bayansal, G. Cankaya, Physica B 405 (2010) 287–290.
[20] E.H. Rhoderick, R. Willams, Metal–Semiconductor Contacts, Clarendon Press, Oxford, 1998.
[21] S.M. Sze, Physics of Semiconductor Devices, 2nd ed., Wiley, New York, 1981.
[22] A. Ziel, Solid State Physical Electronics, 2nd ed., Prentice-Hall, Englewood Cliffs, NJ, 1968.
[23] C.W. Wilmsen, Physics and Chemistry of III–V Compound Semiconductor Interfaces, Plenum Press, New York, 1985.
[24] J.H. Werner, Appl. Phys. A 47 (1988) 291–300.
[25] K.K. Kwok, Complete Guide to Semiconductor Devices, McGraw-Hill, New York, 1995.
[26] R.T. Tung, Phys. Rev. B 45 (1992) 13509–13523.
[27] C.R. Crowell, Solid-State Electron. 20 (1977) 171–175.
[28] S. Karatas, A. Turut, S. Altindal, Nucl. Instrum. Methods Phys. Res. A 555 (2005) 260–265.
[29] K.P. Pande, C.C. Shen, J. Appl. Phys. 53 (1982) 749–753.
[30] G. Cankaya, N. Ucar, E. Ayyildiz, H. Efeoglu, A. Turut, S. Tuzemen, Y.K. Yogurtcu, Phys. Rev. B 60 (1999) 15944–15947.
[31] M. Cakar, C. Temirci, A. Turut, G. Cankaya, Phys. Scr. 68 (2003) 70–73.
[32] W. Mönch, Semiconductor Surfaces and Interfaces, 2nd ed., Springer, Berlin, 1995.
[33] H. Müller, R. Trommer, M. Cardona, Phys. Rev. B 21 (1980) 4879–4883.
[34] I. Gorczyca, N.E. Christensen, M. Alouani, Phys. Rev. B 39 (1989) 7705–7712.
[35] N. Bouarissa, Solid-State Electron. 44 (2000) 2193–2198.
[36] I.-H. Choi, P.Y. Yu, J. Phys. Chem. Solids 62 (2001) 825–827.
[37] M.K. Hudait, S.B. Krupanidhi, Mater. Sci. Eng. B 87 (2001) 141–147.
[38] H.C. Card, E.H. Rhoderick, J. Phys. D 4 (1971) 1589–1601.
[39] S. Ashok, J.M. Borrego, R.J. Gutmann, Solid State. Electron. 22 (1979) 621–631.
[40] S. Pandey, S. Kal, Solid State Electron. 42 (1998) 943–949.
[41] E.H. Nicollian, J.R. Brews, Metal–Oxide–Semiconductor Physics and Technology, Wiley, New York, 1982.
[42] A. Ahaitouf, E. Losson, A. Bath, Solid-State Electron. 44 (2000) 515–520.
[43] H. Yamagishi, Jpn. J. Appl. Phys. 27 (1988) 997–1001.
[44] A. Sellai, P. Dawson, Surf. Rev. Lett. 13 (2006) 273–278.
[45] M. Mamor, A. Sellai, J. Vac. Sci. Technol. A 26 (2008) 705–709.
[46] A. Sellai, Z. Ouennoughi, Mater. Sci. Eng. B 154–155 (2008) 179–182.